J.E. Evans, J. Capon, and D.A. Shnidman

Multipath Modeling for Simulating the Performance of the Microwave Landing System

The Microwave Landing System (MLS) will be deployed throughout the world in the 1990s to provide precision guidance to aircraft for approach and landing at airports. At Lincoln Laboratory, we have developed a computer-based simulation that models the performance of MLS and takes into account the multipath effects of buildings, the surrounding terrain, and other aircraft in the vicinity. The simulation has provided useful information about the effects of multipath on MLS performance.

The Microwave Landing System (MLS) is a new precision approach and landing navigation system that aircraft will soon be using at major and small airports. MLS is a navigation system that operates conventionally: an aircraft determines its location by an on-board analysis of measurements that the vehicle makes of signals that are emitted from the ground. In particular, the aircraft calculates its elevation, azimuth, and distance with respect to separate elevation, azimuth, and distance-measuring-equipment (DME) [1] transmitters on the ground. MLS thus provides navigation information that pilots can use to land their aircraft, even in adverse weather conditions.

Endorsed by the International Civil Aviation Organization (ICAO), MLS has the following improvements over the current Instrument Landing System (ILS).

Precision guidance and range information over a wide geographic area. With such information, pilots can land their aircraft under instrument flight rules (IFR), even in adverse weather conditions. Also, air traffic controllers can instruct pilots to use curved and segmented approach patterns in order to increase runway efficiencies and minimize noise levels around airports.

Electronic guidance using scanning microwave beams. Scanning microwave beams are much less susceptible to reflections from irregular terrain than are ILS beams, which require a smooth ground surface. Hence, for small airports and heliports situated in hilly regions, MLS offers affordable approach and landing navigation.

In adverse weather conditions, MLS is often the only source of accurate navigational information that is available to pilots who are about to land their aircraft. Thus it is imperative that MLS provide virtually error-free performance.

The basic accuracy of the system has been validated by many tests. In addition, real-time monitoring of performance by receivers in the runway area has further verified MLS's accuracy. Thus, because other system errors have been dealt with successfully, multipath is the major potential cause of unacceptable angle and range errors. The major multipath sources of errors for MLS are signal reflection and diffraction. Figure 1 illustrates these two types of scattering phenomena. Note that specular reflections can occur off the terrain, physical structures such as buildings, and other aircraft. Shadowing, which causes beam diffraction, can result from runway humps, other aircraft, and buildings.

The Lincoln Laboratory program that analyzed the effects of multipath on MLS performance commenced with the Laboratory's participation in a NATO study [2] that looked at candidate MLS concepts for military use. During the study, it became clear that multipath would play an important role in distinguishing between various candidates and in the use of the selected system. The study also revealed that a substantive test program was needed to achieve a real-

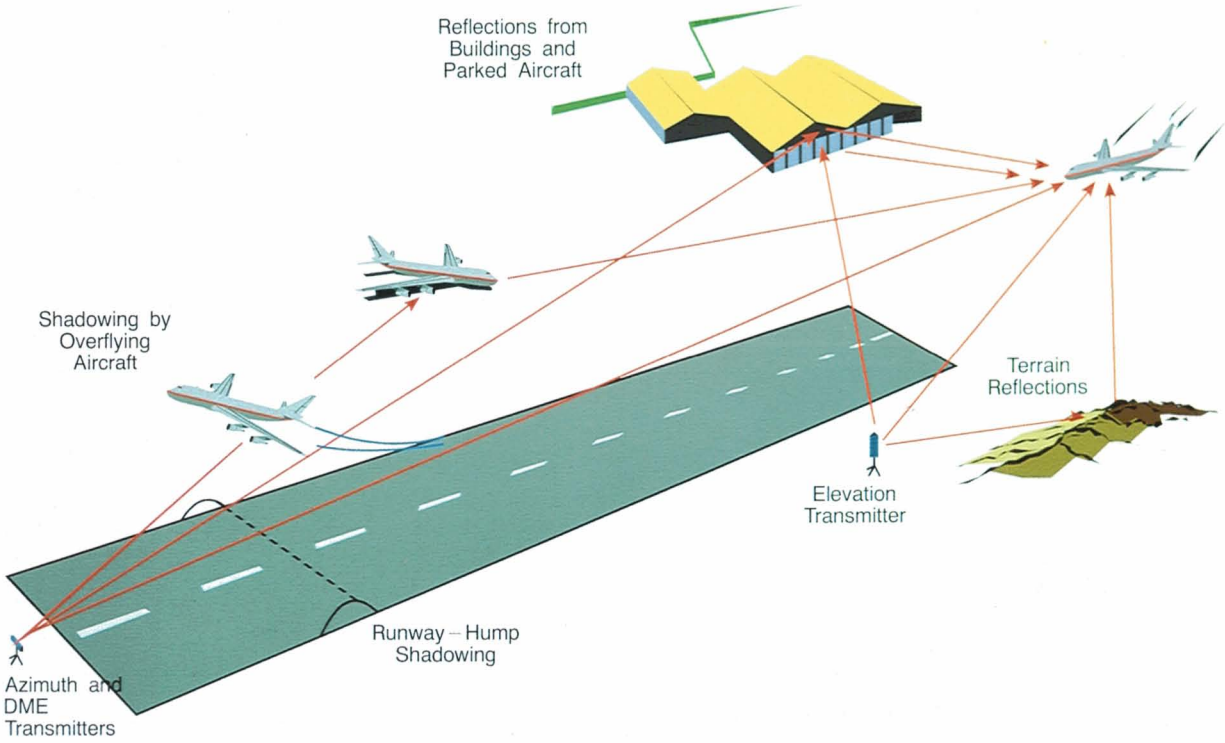

Fig. 1—MLS multipath phenomena.

istic multipath-performance evaluation. Subsequently, the Federal Aviation Administration (FAA) commissioned Lincoln Laboratory to develop a multipath model for comparing various MLS techniques that were under study by the FAA and/or proposed to the ICAO. The model, which was used extensively as an assessment tool in ICAO's evaluation [3, 4], is now being used to perform a variety of analyses for supporting MLS deployment. In particular, the following issues are being investigated:

(1) Where should MLS be sited?
(2) How should taxiing aircraft and other vehicles in the vicinity of MLS be constrained?
(3) Which of the various types of MLS ground equipment should be used at a given site?
(4) What impact would proposed airport changes (e.g., the addition of a building) have on MLS data quality?

Note that to investigate such issues by direct measurement at major airports is logistically very difficult and more costly than by computer-based simulation.

This article describes the methodology used to develop a simulation that models both MLS performance as well as the various multipath phenomena that affect MLS performance. The experimental validation of the simulation is discussed as well as the simulation's application for investigating locations where wide-body aircraft near the runway may cause unacceptable levels of reflection multipath.

Simulations for specific situations have four principal elements:

(1) an airport model that contains the locations and characteristics of reflecting and shadowing obstacles, terrain features, and the MLS antenna locations;
(2) a flight-profile model that describes the routes flown by aircraft;
(3) a multipath model that takes into account the various reflection and diffraction paths and determines the radio signals that are received by the receiver for

each evaluation point along a flight path; and

(4) a system model that determines the multipath system error for the specified MLS ground equipment and receiver processing algorithms used.

This article will focus on elements (3) and (4). The first two elements will be discussed briefly in the context of specific issues that concern multipath sources and receiver modeling.

The development of our simulation was guided by a need to address the error sources relevant to MLS. (This approach contrasts with generic simulations that can be used to simulate the performance of all surveillance and navigation systems.) Therefore, this article is organized in the following way. The section "MLS Features" describes the key attributes of the Time Reference Scanning Beam (TRSB) system, which the ICAO adopted as its standard MLS. The multipath-mitigation features of TRSB are discussed. Next, the section "Multipath Model Features" presents the key model features and gives examples of the experimental validation of the system for the various multipath sources. The section "MLS Model Features" then discusses the validation of the receiver portion of the TRSB system model. We validated the model by comparing its output with the measured antenna patterns and the results of bench tests on actual receivers. The section "Simulation Applications" gives an example of the application of the simulation in addressing a multipath issue of current concern. Lastly, the section "Conclusions" summarizes our results.

For two reasons we go into greater detail in this paper than is customary in a review article. First, multipath is a problem for a number of FAA surveillance and navigation systems that operate in the microwave bands. Our multipath model and the modeling insights gained in our research are applicable to a number of these systems. Second, the military has been increasingly interested in bistatic surveillance systems, in which the transmitter and receiver are located separately. MLS multipath effects can be regarded as a special case of bistatic scattering. Hence the model described in this article might be a useful starting point for a systems analysis of bistatic scattering.

We should note that in our research it was important to minimize the simulation computation time to a level that was practical and feasible in the context of the computers that were available in the mid-1970s. This requirement led us to adopt a ray-theory model for handling all of the reflection and diffraction phenomena of concern.

MLS Features

To provide the framework for a later discussion of multipath modeling, this section describes MLS and explains characteristics of the system's multipath-related errors.

The typical MLS region of coverage is a distance defined up to a range of 20 nmi by an azimuth sector of ±40° around the runway centerline and an elevation sector of +1° to +20°. Outside these sectors, separate transmitters located to the side and back of the MLS transmitters warn pilots that they are flying to the left of, to the right of, or in back of the region of coverage.

The DME currently in use is a high-precision version of the conventional L-band DME, which was used for en route distance measurements for many years. The high-precision DME modifies the leading edge of the DME pulses to improve the system's multipath immunity and basic accuracy [5].

MLS obtains the angular locations of aircraft by electronically scanning a ground antenna's fan beam to and fro so that the time separation of the received beam at the aircraft is proportional to θ_0, which is defined as the angle between the runway centerline and an aircraft's position (Fig. 2). As a first approximation, the received beam envelope is equivalent to the ground-antenna pattern as a function of θ. (If the ground antenna rotated physically, the received envelope would be identical to the antenna pattern. In electronically scanned arrays, however, the received envelope is not exactly identical to the antenna pattern because the arrays typically have sidelobes that vary with scan direction resulting from phase-shifter quantization effects.)

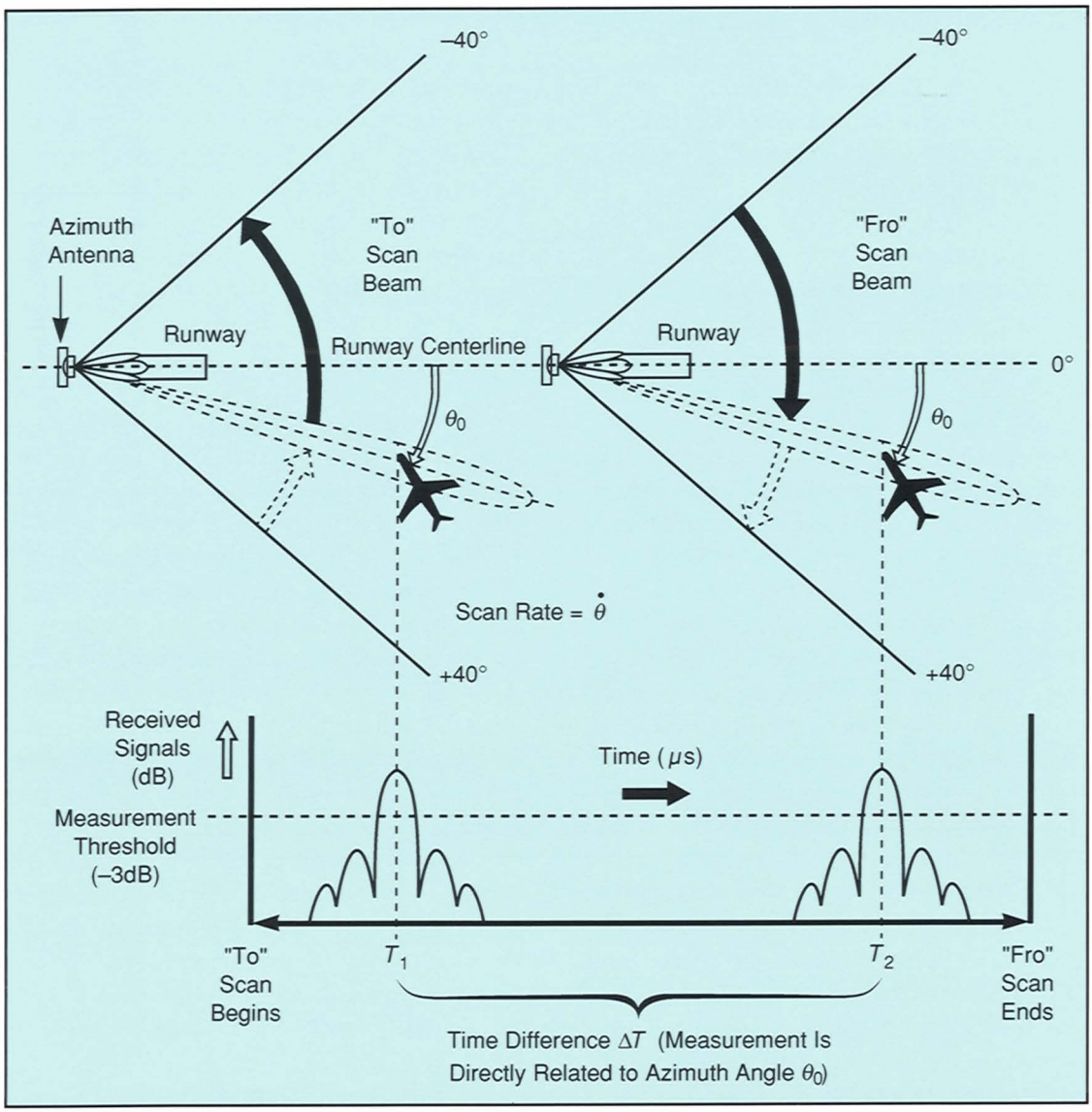

Fig. 2—TRSB bidirectional scan format. Note that ΔT *is directly related to the azimuth angle* θ_0.

The ground antennas typically have a beamwidth of 1° to 3° between the mainlobe's half-power points, and sidelobes that are approximately –25 dB with respect to the mainlobe's peak. Because the angle guidance signals are radiated at a high frequency (C-band), we can readily design the antenna so that its radiation is confined to the desired coverage region. For example, to minimize ground reflections, the elevation pattern of the azimuth antenna can be designed to roll off rapidly at the horizon. The airborne receiver determines the beam centroid to a fraction (typically 5%) of the beamwidth by locating the –6-dB points on either side of the beam or by using a split-gate tracker [6].

Let us now consider the effects of multipath on a received signal. When a multipath signal is at a scanned angular coordinate different from that of the direct signal, the received waveform will consist of the coherent superposition of the two beam envelopes such that the centroids of the received beam shapes may no longer be at the appropriate locations. For both the centroid and split-gate types of receivers, the error that results from multipath depends critically on the multipath source's angular location with re-

spect to the angular location of the receiving aircraft in the scanned angle coordinate:

(1) *In beam.* When the angular separation (δ) between the direct and multipath signals is less than 1.5 transmitter beamwidths (θ), the multipath error can be as large as approximately $0.5R\theta$, in which R is the multipath amplitude divided by the direct-signal amplitude. For small δ, the worst-case error is proportional to δR.

(2) *Out of beam.* When $|\delta| > 1.5\theta$, the direct signal of the received envelope is perturbed by sidelobes that result from beam scattering by the multipath source. In this situation, the worst-case error is approximately $R\eta\theta$, in which η is the sidelobe amplitude ratio for the transmitter antenna. The MLS tracking and acquisition logic may attempt to start a track of a multipath signal if η is greater than unity and if the multipath condition exists for a long period of time, e.g., 20 s when MLS has been tracking the direct signal for at least that amount of time.

Similarly, the DME measurement is accomplished by delay-and-compare processing [5] on the leading edge of the DME pulse such that multipath delays (τ) greater than approximately 300 ns will not cause errors. For shorter multipath delays relative to the direct signal, the worst-case error is approximately given by $R\tau$.

The above multipath error characteristics of MLS have been important in guiding our multipath modeling effort. In particular, we note that out-of-beam multipath is of little concern for the angle guidance subsystems unless the multipath level exceeds that of the direct signal for a long period of time, e.g., for more than 5 s. Because multipath sources in airport terminal complexes are typically located in out-of-beam areas, low-level reflections from the many small objects (e.g., luggage carts) in those areas are not of operational concern. Hence these small objects need not be considered in the modeling effort. Similarly, scatterers (e.g., the flat terrain in front of an azimuth array) that give rise to in-beam multipath at a very small separation angle typically cause only small guidance errors. Thus those types of scatterers need not be modeled

Table 1. Principal MLS Multipath Sources of Concern

Azimuth
- Building reflections and diffraction when aircraft are not on runway centerline
- Aircraft reflections (especially when the scattering source is near the approach end of the runway)
- Shadowing by taxiing and overflying aircraft
- Shadowing by small objects in front of the antenna
- Scattering from irregular terrain in front of the antenna

Elevation
- Reflections from aircraft and buildings in coverage region
- Reflections from sharply rising terrain
- Building shadowing (when aircraft are not on runway centerline)

DME
- Reflections from scatterers with multipath delays between 20 ns and 300 ns

very accurately. Given the above error characteristics, Table 1 summarizes the scatterers of major concern.

Multipath Model Features

This section describes some of the salient features of the models we use to compute reflected and diffracted signals. Because the detailed mathematics of the models are available in a series of Lincoln Laboratory reports [3, 4, 7], our objective in this article is to present some of the principal innovative ideas in the modeling and to show examples of the model validation.

First, however, a few words about the outputs of the scatterer models are in order. For a given geometry that involves a transmitter, a receiver, and signal-scattering objects, each received signal component is characterized [3, 4, 8] by its

(1) amplitude (ρ),
(2) RF phase change due to scattering (ϕ),
(3) time delay relative to the direct signal (τ),
(4) elevation and azimuth relative to the ground antenna (α_t, β_t),
(5) fractional Doppler shift due to the motion of the receiver (ω_{sd}), and
(6) arrival angles at the aircraft relative to the vehicle's velocity vector (α_r, β_r).

(Note that for a given transmitter-receiver-scatterer geometry, there may be a number of received signal components due to the effects of secondary paths that involve ground reflections and/or the decomposition of a given scatterer's return into several scattered or diffracted rays.) We assume that the receiver and the scatterers are far enough from the ground antenna so that the system model can represent the actual antenna patterns at each instant of time during the ground antenna scan by using the angles α_t, β_t, α_r, and β_r. In addition to accounting for Doppler shift of the received signal structure due to receiver motion (a small effect with the ICAO-standard MLS), the term ω_{sd} handles changes in the received signal phase between successive antenna scans.

Another key element of our propagation model is that it takes into account the multiple-bounce reflection paths that can result from buildings, aircraft, and the surrounding terrain. This feature is important because ground reflections can substantially reduce the effective azimuth and DME direct-signal level at low altitudes where the MLS accuracy requirements are most demanding. The model handles multiple-bounce effects by computing three additional signal components that correspond to the three additional paths that involve ground (G) reflections between the transmitter (T), scattering object (O), and receiver (R). That is, in addition to the standard T-O-R path, the paths T-G-O-R, T-O-G-R, and T-G-O-G-R are considered. To keep the entire computation manageable, we assume that the terrain of concern for these secondary ground reflections is flat so that the conventional method of images [7] can be used.

Specular Ground Reflection

Earlier, we noted that irregular terrain presents an important and direct multipath challenge to the performance of MLS. (As discussed above, reflections from homogeneous flat terrain is a secondary challenge. When the terrain is approximately flat and homogeneous, a standard simplified model for terrain reflections can be invoked [9].) In irregular terrain conditions, the ground is considered to be a composite rough surface (as discussed by Beckmann [10]) that has a small-scale roughness superimposed on a large-scale roughness. The large-scale roughness, which describes a region's topographical features, is modeled by dividing the ground surface of concern into a number of triangular or rectangular plane surface elements, each with a homogeneous dielectric constant. The small-scale roughness of the surface elements is assumed to have a Gaussian height distribution with rms roughness σ_h. We further assume that σ_h is smooth enough so that we can apply the Beckman-Spizzichino [10] approximation, in which the effect of the small-scale roughness is to reduce the reflected signal for that plate.

Because the elevation patterns of the MLS antenna roll off rapidly near the horizon, ground reflections are of concern principally at very low elevation angles. At such angles, the Fresnel-zone ellipses are often highly elongated so that

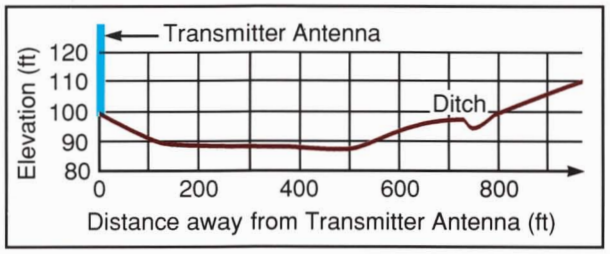

Fig. 3—Terrain height profile of Fort Devens, Mass., golf course.

Fresnel diffraction is no longer valid. Thus, in the general case, a received signal component is computed for each surface element by using a slightly simplified full Fresnel–Kirchoff diffraction formula. (The main simplification is that the integration is performed over a rectangular region that corresponds to 2.8 Fresnel zones. This choice of region has been shown to compare well with closed-form results for an infinite conducting plane in a variety of transmitter-receiver geometries [7].)

We conducted extensive field tests to characterize how well our model represented the irregular terrain. The tests were experimentally challenging because there were sometimes a number of scattered signals whose angular separation in elevation (i.e, α_t) was less than the elevation beamwidth of the measurement system. Consequently, to analyze the experimental data we used several techniques [11] for estimating the high-resolution power spectra for the model outputs.

Figure 3 shows one of the experimental sites, which is characterized by both downhill and uphill terrain with cross-slopes at several locations. We approximated the site with 17 rectangular plates that corresponded to the site's large-scale topographical features. For the terrain of Fig. 3, Fig. 4 compares the model's data with C-band measurements taken with a 60-λ wave-front sampling aperture [12]. In Fig. 4, BS is the classical beam-forming estimate, ME is the maximum-entropy least-squares estimate, and ML is the maximum-likelihood estimate [11]. Note that both the measured and simulated estimates suggest the presence of approximately two scattered specular returns in addition to the direct signal.

Building Reflections

To model buildings and hangars, we use one or more rectangular plates, each of which has a specified small-scale roughness height, a dielectric constant, and, in order to account for sloped roofs, a factor that represents the plate's tilt from the vertical. Each plate causes four scattered signals resulting from the secondary terrain-reflection effects discussed earlier.

We now consider the computation for a single plate with a given transmitter-receiver position. By invoking Babinet's principle [7], we can show that the scattered signal for a given plate can be approximated by a product of Fresnel integrals that corresponds to the horizontal and vertical integration over the plate. This separable-

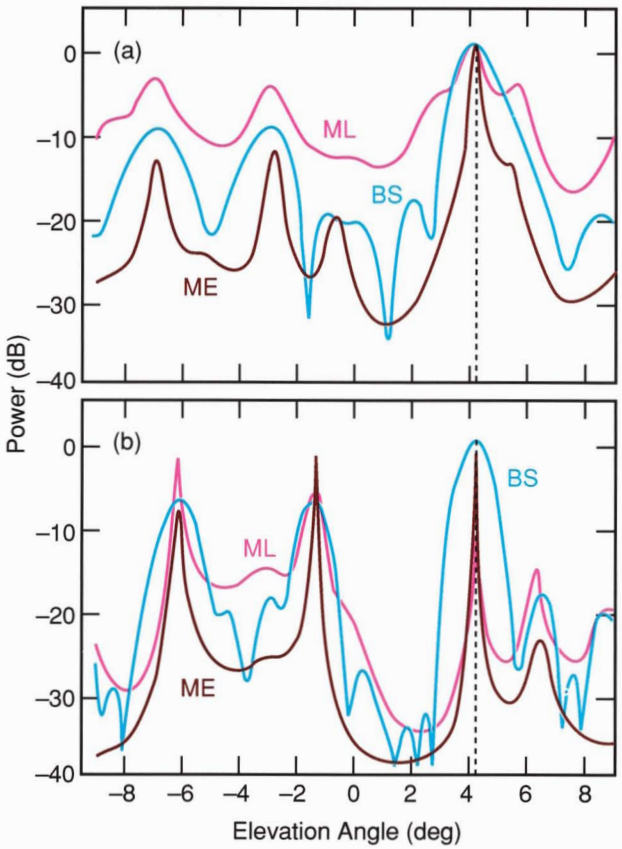

Fig. 4—Comparison of C-band power spectra from (a) field measurements and (b) computer model for the terrain of Fig. 3.

Fresnel-diffraction assumption greatly increases our computational efficiency because it allows the use of standard subroutine packages that contain efficient numerical routines for the evaluation of the integrals.

Our model has been validated in both large-scale qualitative and detailed quantitative tests. The basic model predicts the occurrence of sizable building reflections only with building geometries that yield specular reflections for the given transmitter-receiver locations. This prediction, which was initially verified in tests with a receiver on a moving van at Logan International Airport in Boston [13], was confirmed in subsequent testing with moving vans and aircraft at National Airport in Washington, D.C.; Philadelphia International Airport; Wright Patterson AFB in Ohio; Tulsa International Airport in Oklahoma; and Kennedy Airport (JFK) in New York City [3, 14, 15].

Using an instrumented van parked at a surveyed point, we took multipath amplitude measurements as a function of receiver height and compared the measurements with our model's predictions. Figure 5 shows the comparison for reflections from a Delta Airlines hangar at Logan Airport. In this case, the transmitter and receiver were respectively 1,025 and 675 ft from the hangar, and the transmitter-to-hangar angle of incidence was 45° [13]. Similar agreement between real and simulated data was also obtained in tests involving the hangars at JFK airport [14, 15].

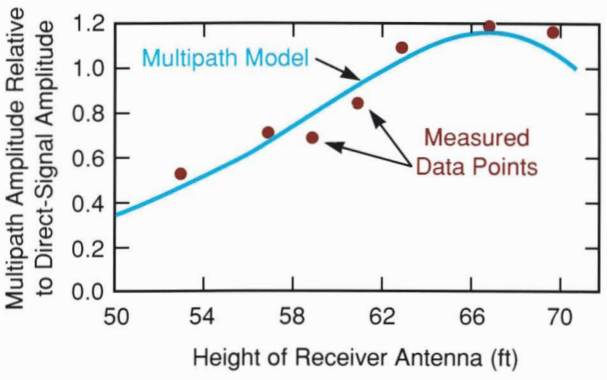

Fig. 5—Comparison of multipath model with C-band measurements for the Delta Airlines hangar at Boston's Logan International Airport (8 December 1974).

We should note that extensions to the model described above would be useful. A survey to determine the nature of the building-reflection phenomena at eight major U.S. airports found that many of the large buildings at the airports had walls or doors made of vertically corrugated metal in which the surface period of the corrugations was greater than a signal wavelength at C-band [8, 16]. Such surfaces act as a diffraction grating in which reflections occur at the specular angle and at angles that correspond to solutions to the classical grating equation. Unfortunately, the shape of the corrugations is such that either laborious numerical calculations or experimental measurements must be made to determine the signal's power in each scattered mode as a function of the angle of incidence. Furthermore, the plate-computation model will have to be augmented to predict accurately the extent of the reflection region for each reflection mode that does not correspond to the classical specular reflection.

Aircraft Reflections

Reflections from aircraft on the ground are of potential concern because these scatterers are often situated on taxiways close enough to the runway so that the reflected signal causes in-beam multipath. Furthermore, aircraft surfaces are made of curved metal, which scatters beams over a wide range of angles and thus creates a larger region of specular multipath than would be produced by flat plates of the same sizes. Based on the results of our field tests and published data for aircraft cross sections versus aspect angles, we conclude that only the tail fin and fuselage of an aircraft need to be considered for our purposes.

Thus, following a suggestion by H.A. Wheeler [17], we modeled both the tail fin and fuselage with portions of cylinders. The reflection levels were estimated by taking the product of a Fresnel integral that corresponded to integration along the cylinder, and a term to account for ray divergence. The computation of ray divergence by integrating around a curved surface is a formidable task. Wheeler, however, cleverly noted that he could accomplish the integration

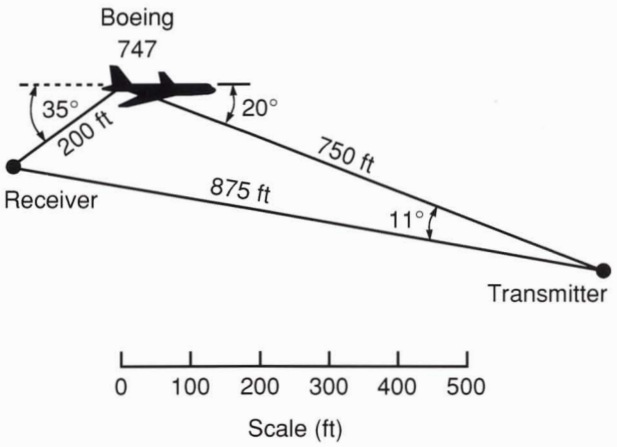

Fig. 6—Geometry for 747 aircraft at Boston's Logan International Airport (12 December 1974). Note that because of the curvature of the aircraft's tail fin, the angle of incidence is not equal to the angle of reflection.

for metallic cylinders by using the closed-form generalized divergence formula of Riblet and Barker [18].

We validated our model by a series of experiments (often in the middle of the night) that involved parked wide-body aircraft at Boston's Logan Airport. For those experiments, Fig. 6 shows the geometry of the transmitter and receiver that were used to take measurements of reflections off the tail section of a 747 aircraft. Note that the angle of the incoming ray as referenced to the centerline of the aircraft is 20°, and the angle of the outgoing ray is 35°. The difference results from the curvature of the aircraft's tail. For the geometry of Fig. 6, Fig. 7 compares the multipath measured levels with the simulated levels. We obtained similar measurements and results for DC-10 and 727 aircraft [7, 13].

Shadowing by Aircraft or Structures near the Line of Sight

Shadowing by obstacles near the transmitter-to-receiver line of sight (LOS) causes multipath errors through two mechanisms. Because of shadowing,

(1) the direct signal might be attenuated, thus causing an increase in the relative amplitude of (and error due to) multipath signals, and
(2) the transmitted wave front might be distorted so that angular errors are directly produced even though little or no attenuation of the direct signal occurs.

Much of the existing literature on shadowing involves radio communication links in which only mechanism (1) was of concern. Thus many radar and navigation system engineers have been surprised to find that sizable angular errors can occur in situations in which the transmitter-to-receiver LOS is not blocked.

We model all shadowing profiles as a collection of flat rectangular plates. For buildings, these plates are analogous to the plate models used for scattering computations. For aircraft, an appropriate plate collection for each viewing angle is chosen; i.e., the front-to-back and top-to-bottom profiles consider the fuselage and wings while the side profile considers the tail fin and fuselage. The user specifies the type of the shadowing aircraft and its movement characteristics; the model then determines an appropriate plate collection for the given shadowing geometry. Thus the diffraction computation reduces to a calculation of separate signals for each of the rectangular plates.

The key point in obtaining a ray-theory representation of the diffracted signal is the following: in determining the number and location of diffracted rays, the principal factor is the variation of the diffracted signal phase as a function of the positions of each of the radiating elements in the aperture of the ground array antenna. Thus the basic idea is to represent the diffracted signal as

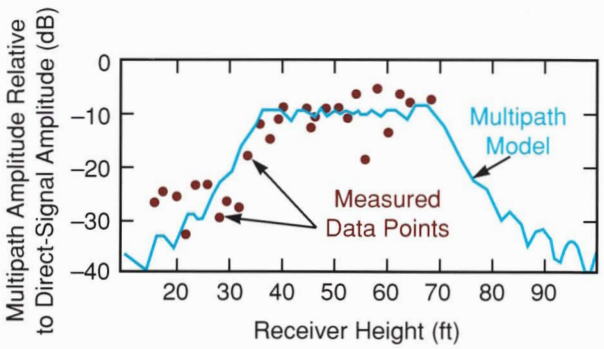

Fig. 7—Comparison of multipath model with C-band measurements for the geometry of Fig. 6.

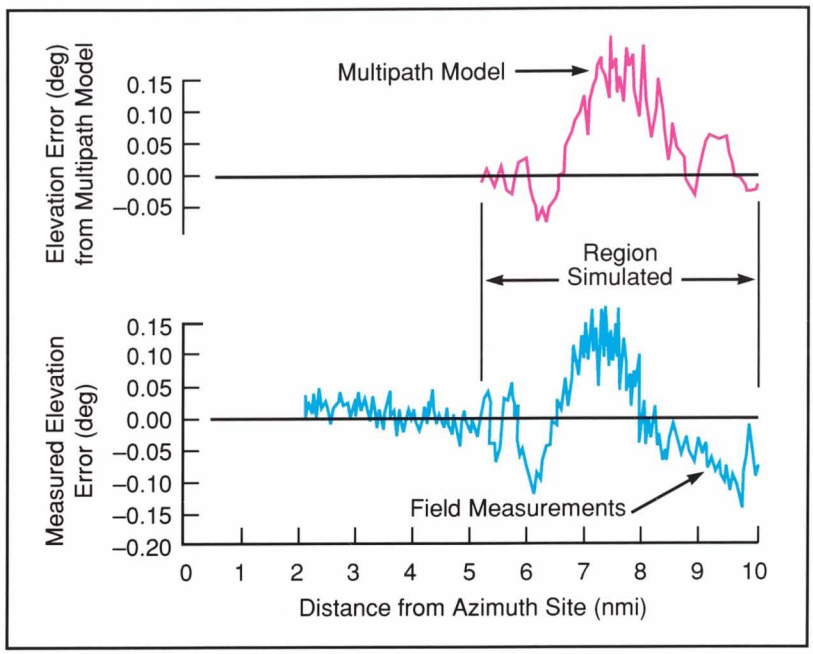

Fig. 8—Comparison of multipath model with field measurements for an aircraft approach at JFK Airport in New York City. The approach was off the runway centerline and shadowing was caused by a large hangar near the MLS elevation antenna.

a Fresnel integral that is a function of the radiating elements' positions in the scanning dimension of the antenna's aperture. (For azimuth arrays, the position is horizontal. For elevation arrays, the position is vertical.) Using standard expansions of the Fresnel integral, we then approximate the integral representation with a sum of plane waves. It can be shown [19] that this procedure yields a ray representation that is a function of the shadowing plate's rectangular size and the LOS. Depending on the size of the obstacle in the coordinate being scanned, one, two, or even three diffraction rays may be created by a given plate.

Figure 8 is a comparison of our model's results with elevation-error measurements of a flight at JFK Airport. The flight, which was off the centerline of the runway, was shadowed by a large hangar that was near the MLS elevation antenna [3]. Figure 9 presents an example of shadowing caused by an airborne aircraft at the FAA Technical Center [3] in Atlantic City, N.J. Given the likelihood of shadowing at major airports, it is important to note how well the output of our model agrees with the experimental data in both of these very different situations.

Humped-Runway Shadowing

When an aircraft is about to touch down, humps in the runway can shadow the vehicle's receiver from the azimuth transmitter or DME. This condition causes a significant loss in the direct signal that the landing aircraft receives.

Initial solutions modeled humps as knife-edge creases in the ground. The representation was simplistic in not taking into account the fact that forward reflections can occur off both sides of a hump, not just the side facing the transmitter. Consequently, we adopted the work of Wait and Conda [20], who modeled humps as infinite dielectric cylinders. Wait and Conda showed that they could represent the diffracted signal as the sum of knife-edge diffraction (i.e., a Fresnel integral) and a correction term that takes into account the radius of curvature of the hump and the dielectric constant of the hump's material. Because the radii of runway humps are con-

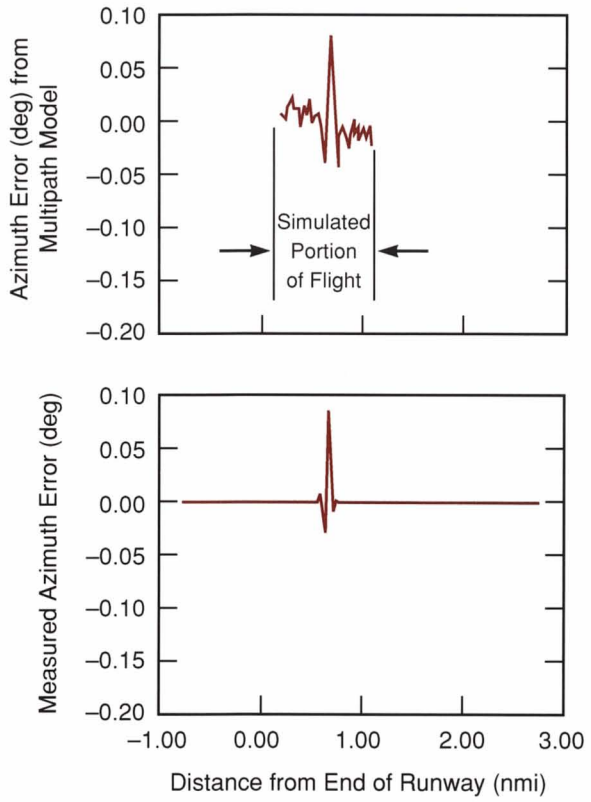

Fig. 9—Comparison of multipath model with field measurements taken at the FAA Technical Center in Atlantic City, N.J. Shadowing was caused by an airborne CV-580 aircraft.

trolled to minimize their adverse effects on aircraft, we found that empirical tables could be used to determine the correction term [7] regardless of the transmitted signal's polarization.

It is important to note that the intended use of the Wait and Conda model is within or near the shadowing region. When an aircraft is high enough so that it is not shadowed by any humps, our multipath model reverts to the standard flat-terrain representation, which considers the ground reflection that occurs near the transmitter. In either the hump or flat-terrain case, the effects of shadowing are treated as a change in the complex amplitude of the direct signal.

We validated our model mainly by comparing its output with field data. Figure 10 compares the results of the model with field tests that were taken on the main runway at the Royal Air Establishment in Bedford, England. Although the overall runway profile does not resemble a dielectric cylinder, the model gives excellent results along a considerable length of the shadowed region. Similar agreement between our model and experimental data was obtained from field tests at France's Coulommiers airport [7]. In both the Bedford and French data, the model gave the best results when it used the largest value for equivalent cylinder radius that could be justified by the runway profile.

The above model, which represents a diffracted signal with a single effective-direct-signal ray, may warrant refinement in the future. Normally, the major operational concern would be whether a given geometric configuration yields an adequate SNR when aircraft are at very low altitudes. In such conditions, however, MLS has an ample power budget margin *if* no shadowing is present. Thus we are principally concerned with model accuracy in shadowed regions; in those areas, the single-direct-ray representation described above is adequate. When the receiver is above the geometric shadow region, however, the representation does not adequately handle the effects of a ground-antenna-pattern gain that varies rapidly near the horizon. Therefore, it is desirable to develop a multiray model that accurately represents the elevation-angle (i.e., β_t) distribution of the net received signal inside and outside the geometric shadow region.

MLS Model Features

The MLS model, which is a very straightforward implementation of Fig. 2, computes the beam envelope received by an aircraft as a beam scans by the vehicle. The functional form of the beam wave is determined by the measured or theoretical patterns of the ground antenna of concern. The superimposition of beam patterns that correspond to the various signal paths results in the net received envelope. The remainder of the MLS model parallels the actual microprocessor-based receiver processing that MLS uses. A tracking gate centers on the largest consistent envelope peak and the beam arrival angle is calculated by finding the times at which the leading and trailing edges of the received envelope cross a certain threshold. Various checks and tracking algorithms screen each

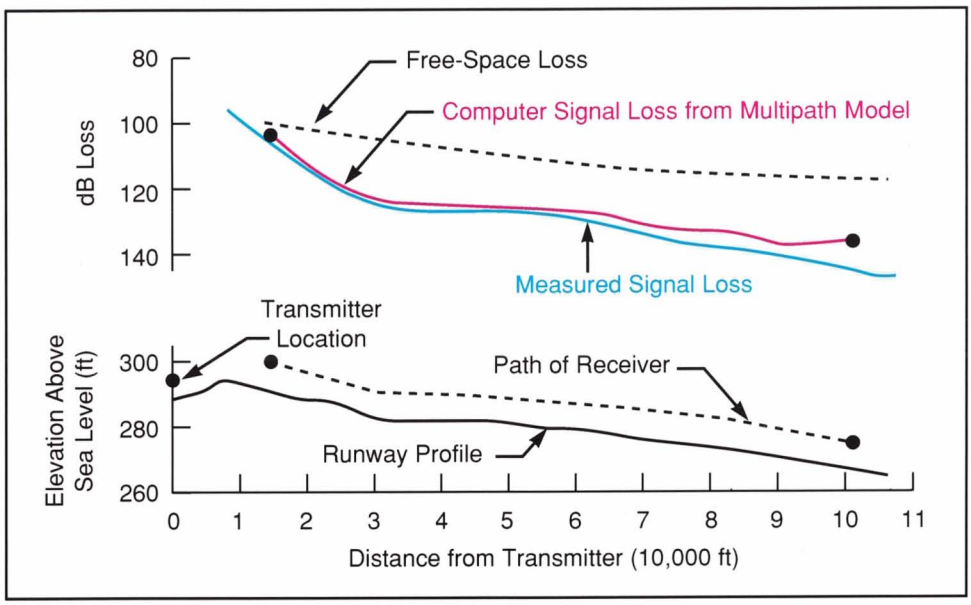

Fig. 10—Comparison of multipath model with C-band measurements taken at the main runway of the Royal Air Establishment in Bedford, England. Shadowing was caused by a runway hump. The transmitter and receiver heights above the local ground level were 4.8 ft and 9.0 ft, respectively.

measurement to ensure that only valid angles and DME measurements are outputted [21].

The performance of the receiver portion of the MLS model was validated primarily at a test facility that the Calspan Corporation developed for the FAA [6]. The Calspan system could inject into an actual MLS receiver a waveform that corresponded to the reception of a direct signal and a single multipath signal. The system had fairly tight control over the characteristics of the direct and multipath signals, e.g., the amplitudes, RF phases, and angular separation between the two signals. Figure 11 compares our MLS model's output with the Calspan Corp. system. Differences between the two sets of data are within the ±0.5-dB tolerance of the multipath-to-direct-signal-level setting of the Calspan Corp. system.

We further validated the MLS model with tests in operational environments similar to that described above. The tests were particularly useful in addressing sidelobe modeling. We found that at a given angular separation from the main-beam location, the sidelobes of an antenna vary with time due to variations in phase-shifter error. Additionally, the phase-shifter scan-control program also causes the errors at a given point in a scan to vary from scan to scan. Thus, it was not clear whether we could accurately represent high-level sidelobe multipath errors with a simple sidelobe model that consisted of an array excitation pattern for the first few sidelobes and a sinusoid with a 1-beamwidth spatial period for the remaining sidelobes.

The simple sidelobe model described above agreed reasonably well with results from field tests at the FAA Technical Center. (The sidelobe model, however, overestimated the magnitude of the multipath error by about 5 dB.) For the FAA tests, large reflecting screens were placed on a runway. The screens caused out-of-beam multipath that was greater than the direct signal over an extensive portion of the runway.

Predicting the effective sidelobe levels for the antennas of various manufacturers presents an ongoing challenge because the static antenna patterns tend to underestimate significantly those sidelobes which are far removed from the mainlobe. The dynamic beam envelopes, on the

other hand, tend to overestimate those same sidelobes.

Simulation Applications

To date, one of the major applications of our MLS multipath simulation has been in determining critical areas where restrictions must be placed on the movement of aircraft and other vehicles to avoid excessive MLS guidance errors. In this section, our discussion will deal only with reflection effects because shadowing effects can readily be addressed by the same method.

One possible way to determine critical reflection areas is to carry out full-scale simulations of aircraft approaches with a scatterer at each possible airport location of concern. This method, however, requires a prohibitively large volume of computer runs because of the numerous multipath scatterer parameters (e.g., aircraft type, truck size), types of ground antenna systems, and different approach parameters (e.g., ground velocity, airborne-antenna pattern, approach angle) that need to be considered. Consequently, we adopted the following two-stage approach:

(1) The worst-case error is determined as a function of scatterer location for fixed ground- and airborne-system parameters. Simple analytical models determine the effects of receiver motion.

(2) Using the worst-case scatterer locations from step (1), we run full-scale simulations. The simulations determine the way in which the different receiver-approach parameters affect the multipath parameters. In addition, the simulations determine the operational nature of the resulting error.

This two-stage approach, which takes advantage of the modular nature of the overall simulation, permits the consideration of a wide range of parameters for all of the principal variables.

We will now illustrate the above approach for the specific case in which reflections off a taxiing aircraft cause azimuth errors for an airborne aircraft just before touchdown. In this example, the largest combined multipath level for fuselage and tail-fin reflections occurs when the taxiing aircraft is turned so that the reflection point is in the middle of the vehicle's fuselage. Using this knowledge, we can orient the taxiing aircraft to yield the maximum multipath level at each point on the airport surface at which the worst-case error is to be calculated. The worst-case errors are individually computed as the sum of the absolute values of the errors that result from fuselage and tail-fin reflections. (The errors are calculated as the ratio between the multipath level and the direct-signal level. Both the multipath and direct-signal levels take into account ground-reflection effects.)

For the above example, Fig. 12 shows the 0.03°-error contours as a function of aircraft position for a Boeing 747 and 727 aircraft. From the figure, we see that only the 747 aircraft is of

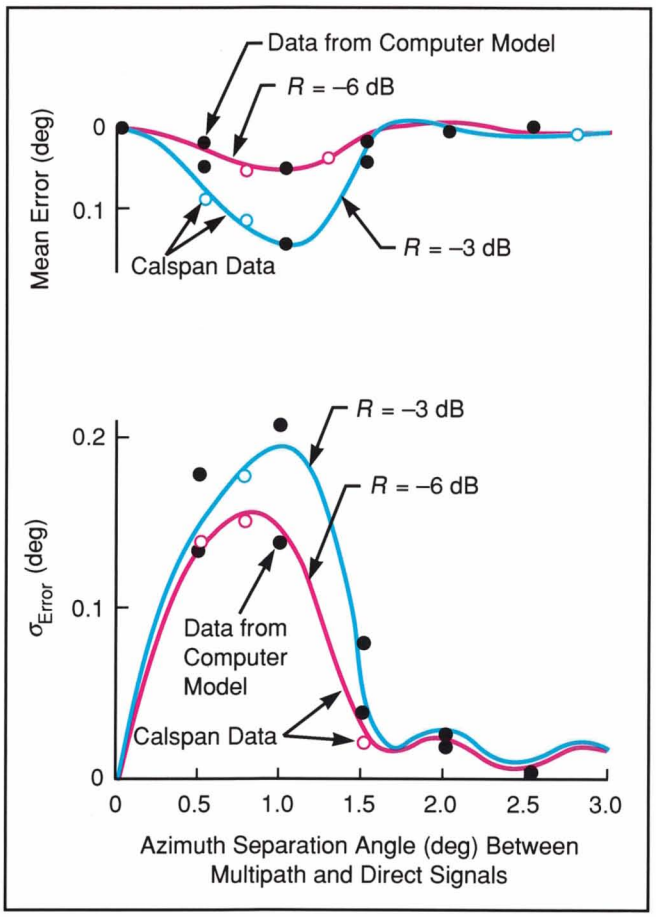

Fig. 11—Comparison of computer model with Calspan data taken at a scalloping frequency of 0.6 Hz. The mean error and standard deviation in error are calculated with respect to the RF-phase difference. R *is the multipath level divided by the direct-signal level.*

concern. It is also important to note that the most severe multipath effects occur when the taxiing aircraft are within a holding area adjacent to the end of the runway.

Because current ICAO guidelines require taxiways that are parallel to a runway to be at least 300 ft from the runway's centerline, Fig. 12 suggests that existing taxiways can be used during MLS instrument approaches. This observation was further confirmed in full-scale simulations in which five worst-case-oriented 747 aircraft were located at points 300 ft from the runway centerline. The vehicles produced maximum multipath levels at 8, 50, 100, and 200 ft above ground level, and the peak azimuth errors encountered during the full simulation run were less than 0.01°. These results confirm the conservative nature of the worst-case-error calculation [8]. It should be noted that 747s located 150 ft off the runway in the middle of the error contour shown in Fig. 12 were found to produce unacceptable errors (0.07°) when the landing aircraft was near touchdown.

Similar calculations for MLS elevation measurements show that the area immediately in front of the MLS elevation system should be kept free of 747 aircraft. However, on the opposite side of the runway, aircraft on the surface may operate freely without any adverse effects [8].

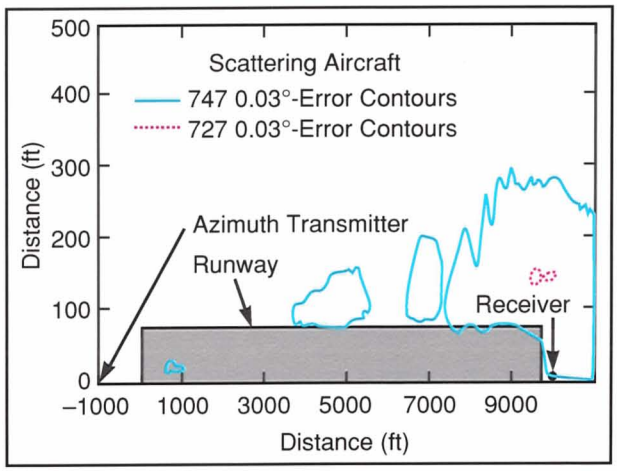

Fig. 12—Plan view of simulated scattering conditions at a hypothetical runway. The simulation was performed for two different types of aircraft: a Boeing 747 and 727. The contours enclose areas where the MLS azimuth error is at least 0.03°. That is, if a taxiing 747 or 727 is inside its respective contour, the azimuth error would be at least 0.03° for an aircraft about to land on the runway. For this particular example, the airborne aircraft is assumed to be approaching along the runway centerline, 11,000 ft from the transmitter antenna and 50 ft above the ground.

Conclusions

This article describes a very ambitious simulation that can handle the full range of multipath phenomena of concern to MLS. We accomplished this comprehensiveness only by carefully considering the MLS error mechanisms at the outset. We then focused the multipath model development and validation to emphasize those factors which were of greatest concern. Fortunately, Lincoln Laboratory personnel were very actively involved in the U.S. and ICAO MLS evaluation programs, which were being conducted throughout the major period when the simulation was developed. Our involvement provided us with the opportunity to interact closely and frequently with a very knowledgeable group that was always available to critique our work. As a consequence of this close scrutiny, the model received extensive validation both by dedicated propagation measurements in a variety of locations as well as in comparison with the results of operationally oriented testing at airports in the United States and abroad.

We would like to call special attention to two particular features of the multipath model that previous work has often ignored. The consideration of ground reflections in determining both the effective direct-signal level and effective multipath-signal levels is especially important at low altitudes, where MLS guidance is particularly critical. Second, the use of a ray-theory model for representing shadowing phenomena permits the consideration of errors that result from wave-front distortion as well as errors that involve losses in the direct-signal level.

Lincoln Laboratory has also used the multipath model with the Mode-S [22] radar system to predict monopulse errors caused by shadowing. Thus the model can readily be adapted for other Mode-S propagation studies. In addition, the scattering assumptions we made are such that the model can also be used to evaluate multipath effects (in particular, angular errors due to

shadowing, and false targets due to reflection multipath) for the ASR-9 (Advanced Surveillance Radar-9) and TDWR (Terminal Doppler Weather Radar) systems.

In the preceding sections, we noted several desirable refinements to the multipath model. Furthermore, we see the need to add the following two capabilities: consideration of out-of-coverage and fly-left/fly-right sector radiation signals, and explicit flagging of low SNR conditions.

Acknowledgments

The models described in this article are the result of several years of research conducted during the 1970s by a dedicated group at Lincoln Laboratory. Principal contributors included Richard Orr, David Sun, Robert Burchsted, Steve Sussman, Samuel Dolinar, Janet Reid, and Carol Martin. Work by Dr. Harold Wheeler of Hazeltine Corporation was very significant in our approach to multipath modeling and in our use of analytical system-error models to complement the results of formal calculations. We also benefited greatly from intense technical interactions with Robert Kelly of Bendix Corp., Mel Zeltser of Hazeltine and MITRE Corp., Lon Sanders of ITT Gilfillin, Paul Fombonne of Thompson CSF, Jack Beneke of Calspan Corp., the United Kingdom MLS group at the Royal Air Establishment in Bedford, England, and the University of Braunschweig in West Germany.

Special mention should also go to the MLS program office of the Federal Aviation Administration. In particular, we thank Frank Frisbie, Joseph DelBalzo, Douglas Vickers, and Gene Jensen for their support and encouragement throughout the MLS development and evaluation period.

References

1. M. Kayton and W.R. Fried, eds., *Avionics Navigation Systems*, John Wiley & Sons, Inc., New York (1969).
2. T. Breien "Computer Analysis of MLS in Multipath Environment," *IEE Conference Publication No. 147* (Nov. 1976).
3. J.E. Evans, S.J. Dolinar, D.F. Sun, and D.A. Shnidman, "MLS Multipath Studies, Phase 3. Final Report, Volume II: Development and Validation of Model for MLS Techniques," *Project Report ATC-88*, Lincoln Laboratory (7 Feb. 1980), FAA-RD-79-21.
4. J.E. Evans, S.J. Dolinar, and D.A. Shnidman, "MLS Multipath Studies, Phase 3. Final Report Volume III: Application of Models to MLS Assessment Issues," *Project Report ATC-88*, Lincoln Laboratory (8 June 1981), FAA-RD-79-21.
5. R.J. Kelly and E.F.C. LaBerge, "Guidance Accuracy Considerations for the Microwave Landing System Precision DME," *Navigation, Journal of the Institute of Navigation* **27,** 1 (1980).
6. J. Beneke, D. Wightman, A. Offt, and C. Vallone, "TRSB Multimode Digital Processor," Calspan Corp. Final Report (Apr. 1978) FAA-RD-78-84.
7. J. Capon, "Multipath Parameter Computations for the MLS Simulation Computer Program," *Project Report ATC-68*, Lincoln Laboratory (8 Apr. 1976), FAA-RD-76-55.
8. J.E. Evans, R.B. Burchsted, J. Capon, R.S. Orr, D.A. Shnidman, and S.M. Sussman, "MLS Multipath Studies, Volume I: Mathematical Models and Validation, Volume II: Application of Multipath Model to Key MLS Performance Issues," *Project Report ATC-63*, Lincoln Laboratory (25 Feb. 1976), FAA-RD-76-3.
9. K.M. Mitzner, "Change in Polarization on Reflection from a Tilted Plane," *Radio Science* **1,** 27 (1966).
10. P. Beckmann, "Scattering by Composite Rough Surfaces," *Proc. IEEE* **53,** 1012 (1965).
11. J.E. Evans, J.R. Johnson, and D.F. Sun, "Application of Advanced Signal Processing Techniques to Angle of Arrival Estimation in ATC Navigation and Surveillance Systems," *Technical Report TR-582*, Lincoln Laboratory (23 June 1982), FAA-RD-82-42.
12. D.F. Sun, "Experimental Measurements of Low Angle Ground Reflection Characteristics at L- and C-Bands for Irregular Terrain," *Project Report ATC-107*, Lincoln Laboratory (1 Nov. 1982), DOT/FAA/RD-81/65.
13. D.A. Shnidman, "The Logan MLS Multipath Experiment," *Project Report ATC-55*, Lincoln Laboratory (23 Sept. 1975), FAA-RD-75-130.
14. "Validation of Computer Simulation by Comparison with Tests at Operational Airports," paper presented by the United States at the International Civil Aviation Organization All Weather Operations Division Meeting, Montreal, Apr. 1978, AWO/78-WP/135.
15. J.E. Evans and P.H. Swett, "Results of L Band Multipath Measurements at Operational United States (U.S.) Airports in Support of Microwave Landing System (MLS) Precision Distance Measuring Equipment (DME/P)," *Project Report ATC-109*, Lincoln Laboratory (23 July 1981), DOT/FAA/RD-81/63.
16. D.A. Shnidman, "Airport Survey for MLS Multipath Issues," *Project Report ATC-58*, Lincoln Laboratory (15 Dec. 1975), FAA-RD-75-195.
17. H.A. Wheeler, "Multipath Effects in Doppler MLS," as contained in Hazeltine Corp. report *Microwave Landing System (MLS) Development Plan as Proposed by Hazeltine Corp. during the Technique Analysis and Contract Definition Phase of the National MLS Development Program* (Sept. 1972), FAA-RD-73-185.
18. H.J. Riblet and C.B. Barker, "A General Divergence Formula," *J. Appl. Phys.* **19,** 63 (1948).
19. J.E. Evans, D.F. Sun, S.J. Dolinar, and D.A. Shnidman, "MLS Multipath Studies, Phase 3. Final Report, Volume I: Overview and Propagation Model Validation/Refinement Studies," Lincoln Laboratory *Project Report ATC-88*, Lincoln Laboratory (25 Apr. 1979), FAA-RD-79-21.
20. J.R. Wait and A.M. Conda, "Diffraction of Electromagnetic Waves by Smooth Obstacles for Grazing Angles,"

J. Res. NBS **63D,** 181 (1959).
21. R.J. Kelly, "Guidance Accuracy Considerations for the Microwave Landing System," *Navigation, Journal of the Institute of Navigation* **24,** 189 (1977).
22. V.A. Orlando, "The Mode S Beacon Radar System," *Lincoln Laboratory Journal* **2,** 345 (1989).

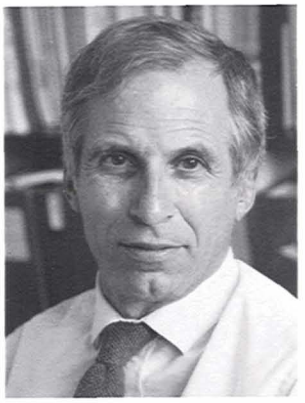

JAMES E. EVANS is Leader of the Air Traffic Surveillance Group at Lincoln Laboratory. The group develops primary-radar weather and aircraft-detection systems for the Federal Aviation Administration. At the Laboratory, Jim has worked on seismic discrimination, ELF communication systems, the Microwave Landing System, high-resolution array processing, and weather radar systems. A senior member of the IEEE, he received an S.B., an S.M., and a Ph.D. from MIT in 1963, 1964, and 1971, respectively. While at MIT, he received the Compton Award and the Carleton E. Tucker award for teaching.

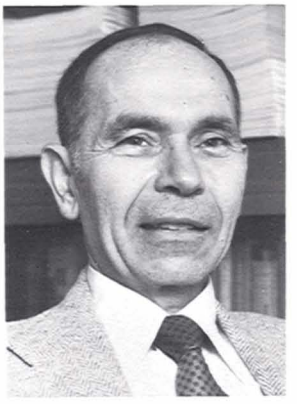

JACK CAPON is a staff member of the Advanced Techniques Group in Lincoln Laboratory's Surveillance and Control Division. A 27-year employee of the Laboratory, Jack has specialized in adaptive array systems. He received the following degrees in electrical engineering: a B.E.E. from the College of the City of New York, an M.S.E.E. from MIT, and a Ph.D. from Columbia University. Jack is a Fellow of the IEEE and the AAAS. He received the IEEE Centennial Medal in 1984, and was elected for two terms to the Board of Governors of the IEEE Professional Group on Information Theory.

DAVID A. SHNIDMAN specializes in antenna research and electronic direction-finding research at Lincoln Laboratory's Surveillance and Control Division. Before joining the Laboratory 18 years ago, Dave worked at Bell Telephone Labs in North Andover, Mass. He received a B.S. and an M.S. in electrical engineering from MIT, and a Ph.D. in applied mathematics from Harvard University. From 1978 to 1979, Dave was the chairman of the Boston Chapter of the IEEE Information Theory Group. He is a member of Eta Kappa Nu, Tau Beta Pi, and Sigma Xi.